Shackleton, N.J., Curry, W.B., Richter, C., and Bralower, T.J. (Eds.), 1997
Proceedings of the Ocean Drilling Program, Scientific Results, Vol. 154

28. MILANKOVITCH-SCALE CLIMATE VARIABILITY RECORDED NEAR THE OLIGOCENE/MIOCENE BOUNDARY[1]

B.P. Flower,[2] J.C. Zachos,[2] and H. Paul[2]

ABSTRACT

High-resolution (ca. 5 k.y.) $\delta^{18}O$ and $\delta^{13}C$ data from Ocean Drilling Program Hole 929A near the Oligocene/Miocene boundary document Milankovitch-scale climate variability from ca. 24.8 to 23.1 Ma. Stable isotopic data based on *Cibicidoides mundulus* better define the timing and magnitude of a $\delta^{18}O$ maximum at ca. 23.9 Ma (event Mi1), and its association with the $\delta^{13}C$ maximum near the Oligocene/Miocene boundary. Mi1 is marked by a gradual increase of 1.2‰ over about 250 k.y. from 23.9 to 23.6 Ma to a maximum of 2.15‰, followed by two rapid (<20 k.y. each) decreases of 0.6‰ at 23.62 and 23.57 Ma. The $\delta^{13}C$ maximum of 1.6‰ is reached at the end of three $\delta^{13}C$ cycles of ca. 400-k.y. period, culminating at 23.65 Ma (coincident with the $\delta^{18}O$ maximum). Oxygen and carbon isotopic data covary through the sequence studied, suggesting a strong relation between organic carbon burial and global climates. However, $\delta^{18}O$ leads $\delta^{13}C$ by about 40 k.y.

Spectral analysis confirms Milankovitch-scale variability in $\delta^{18}O$, $\delta^{13}C$, and percent sand content (>63 µm/g), with a dominant period of about 41 k.y., especially during the 24.0–24.8 Ma interval. Concentration of variance at this period strongly suggests a high-latitude control, probably East Antarctic ice sheet variability.

INTRODUCTION

The Oligocene/Miocene Boundary

Existing paleoclimate records identify the late Oligocene/early Miocene boundary as a time of significant climatic and oceanographic change, with effects seen in both the marine and terrestrial realms. Climatic change at this time was probably influenced by important tectonic developments in the southern hemisphere. Eastward movement of the tip of South America away from the Antarctic Peninsula during the early Oligocene led to a shallow marine connection through Drake Passage between the eastern Pacific and South Atlantic Oceans (Barker and Burrell, 1977; Lawver, 1992). Further opening of the Drake Passage during the late Oligocene deepened the connection and led to the development of the Circumpolar Current (Ciesielski and Wise, 1977; Tucholke and Mountain, 1979). The Oligocene/Miocene boundary coincided with a major hiatus in South Atlantic and Southeast Pacific deep-sea sediments, attributed to intensification of the Circumpolar Current. Isolation and refrigeration of the Antarctic continent by the Circumpolar Current system fostered the development of significant glacial ice on East Antarctica (Kennett, 1977).

Several lines of evidence indicate a brief but major Antarctic glaciation near the Oligocene/Miocene boundary. Oxygen isotope data exhibit a temporary increase at this time (Mi1; Miller et al., 1991). Covariance between low-latitude planktonic and benthic $\delta^{18}O$ suggests an ice volume effect of about 0.8‰ (Wright et al., 1992). A Quaternary calibration of the $\delta^{18}O$/sea level relation (Fairbanks and Matthews, 1978) would suggest about a 70-m fall in sea level, but this may be an underestimate because the middle Tertiary calibration may have been significantly different (Miller et al., 1991). Carbon isotope records also show a maximum at this boundary (Shackleton et al., 1984; Miller and Fairbanks, 1985; Miller et al., 1988; Miller et al., 1989; Wright and Miller, 1992), an event that is well-calibrated to the geomagnetic polarity time scale (C6C–C6B) and to biostratigraphic datum levels.

Sedimentologic data from the CIROS 1 drill hole, McMurdo Sound, record two periods of Oligocene glaciation, from ~36 to 34.5 Ma and from 30.5 to 22 Ma (Barrett et al., 1989). A period of glacial marine sedimentation in the early Oligocene was confirmed in the Prydz Bay sector of the Southern Ocean (Barron et al., 1991) and on Kerguelen Plateau (Breza and Wise, 1992; Zachos et al., 1992). However, there is only limited evidence for glacial marine sedimentation near the Oligocene/Miocene boundary in the Ross Sea (Leckie and Webb, 1983). In this paper, documentation of climatic responses to Milankovitch-scale orbital forcing provides additional evidence of Antarctic glaciation near the Oligocene/Miocene boundary. In the following section, we review how climatic responses at periods indicative of high-latitude processes point to polar ice sheet variability.

Milankovitch Periodicities in the Quaternary

The climate of the mid- to late Quaternary (600–0 ka) has been shown to be dominated by fluctuations with periods at 23, 41, and 100 k.y. (e.g., Mesolella et al., 1969; Broecker and van Donk, 1970; Hays et al., 1976). These periods are associated with variations in Earth-Sun parameters that control insolation on the Earth: precession, obliquity, and eccentricity, respectively (e.g., Berger, 1977). The 23- and 41-k.y. periods exhibit linear responses to orbital forcing (Imbrie et al., 1984, 1992). The 100-k.y. period has been suggested to represent a nonlinear response to the comparatively weak eccentricity forcing. The nonlinearity of the climate system's response is thought to be related to the inertial energy of large, high-latitude ice sheets (Imbrie et al., 1993).

Variations in Earth's obliquity (41-k.y. period) have the greatest effects on insolation in the high-latitude regions as a result of changing seasonality. Conversely, variations in precessional forcing (~23-k.y. period) more directly affects insolation in the low-latitude regions (Ruddiman et al., 1989; Imbrie et al., 1992). This difference in the effective forcing at the different periods has been used to differentiate variability in low-latitude vs. high-latitude regions. For example, changes in dominance of 23-k.y. and 41-k.y. climatic periodicities have been tied to the late Pliocene through Quaternary evolution of the Northern Hemisphere ice sheets and associated changes in sensitivity to high-latitude insolation changes (Ruddiman et al., 1989; Raymo et al., 1989).

[1]Shackleton, N.J., Curry, W.B., Richter, C., and Bralower, T.J. (Eds.), 1997. *Proc. ODP, Sci. Results,* 154: College Station, TX (Ocean Drilling Program).
[2]Institute of Marine Sciences and Earth Sciences Board, University of California, Santa Cruz, CA 95064, U.S.A. flower@earthsci.ucsc.edu

Milankovitch Periodicities in the Tertiary

Attempts to identify a relationship between deep-sea stable isotope records and Earth's orbital parameters in the Tertiary, however, have met with limited success. In general, such studies have been hampered by the unavailability of suitable sedimentary sequences. Factors such as low sedimentation rates, incomplete sequences, and/or poor preservation in older sequences limit the degree to which climate change can be resolved. On occasion, however, with suitable sequences, high quality isotope records have been generated that allow for documentation of high-frequency climate signals. A high-resolution (3-k.y. sampling interval) middle Miocene benthic foraminifer $\delta^{18}O$ record at Deep Sea Drilling Project (DSDP) Site 574, just prior to the major $\delta^{18}O$ increase of >1.0‰ (ca. 14 Ma), revealed a dominant 40-k.y. period (Pisias et al., 1985). This result strongly suggested a link between foraminifer $\delta^{18}O$ and orbital (Milankovitch) forcing during the Miocene. Similar findings for DSDP Sites 526 (Prentice and Matthews, 1988) and 552 (Keigwin, 1987) further document the existence of Milankovitch periodicities in middle to late Miocene oceanic $\delta^{18}O$ records.

For older time intervals, the obstacles to finding suitable sequences for high-resolution study are substantially greater. Nevertheless, a few Eocene and Oligocene high-resolution foraminifer $\delta^{18}O$ records hint at the influence of orbital variations on oceanic $\delta^{18}O$ and ice volume changes particularly in the lower frequency 100- to 400-k.y. bands (e.g., Zahn and Diester-Haass, 1995; Zachos et al., 1996). Spectral analysis of a high resolution benthic $\delta^{18}O$ record from Site 522 revealed the presence of a 41-k.y. periodicity in the early Oligocene, just after the initial appearance of large ice sheets on Antarctica (ca. 35 Ma). Periods of ca. 100 and 400 k.y. have also been detected in Eocene and Oligocene sequences from high-latitude Southern Ocean Sites 744 (Zachos et al., 1996) and 689 (Zahn and Diester-Haass, 1995). In general, however, the sampling of these records was inadequate to fully resolve the precession- and obliquity-driven climate signals (cf. Pisias and Mix, 1988).

Thus, periodicities in a few high-resolution Oligocene and Miocene foraminifer $\delta^{18}O$ records strongly suggest that variations in the Earth's obliquity and eccentricity have been prominent in forcing of climate, even during periods of unipolar glaciation. Unfortunately, however, no single record has been adequate to resolve the full spectrum of orbitally related climate signals observed in Pleistocene sedimentary sequences.

Ceara Rise Depth Transect

Excellent recovery near the Oligocene/Miocene boundary in the Ceara Rise depth transect provides a rare opportunity to develop a high-resolution record that defines the full spectrum of the climate signals. Here, we present $\delta^{18}O$, $\delta^{13}C$ and percent sand (>63 µm/g) records at 5-k.y. resolution from Site 929 (Fig. 1) based on benthic foraminifers that (1) define the timing and magnitude of the Mi1 $\delta^{18}O$ event, (2) document high-frequency, Milankovitch-scale climate variability suggestive of a high-latitude ice volume control, and (3) confirm a south-to-north deep-water $\delta^{13}C$ gradient near the Oligocene/Miocene boundary, indicative of a single Southern Component Water (SCW) source. A companion paper (Flower et al., this volume) presents longer, moderate-resolution isotopic records ($\delta^{18}O$, $\delta^{13}C$, and $^{87}Sr/^{86}Sr$) for the late Oligocene through early Miocene from Sites 926 and 929.

METHODS

Samples were freeze-dried, weighed, soaked, and shaken in deionized water, and washed over a 63-µm sieve; they were then dried and weighed again. Individual benthic foraminifers were handpicked from the 150- to 250-µm size fraction for isotopic analysis. Approximately seven specimens of the benthic foraminifer *Cibicidoides mundulus* were used for each analysis. Specimens for isotopic analysis were sonicated in methanol to remove adhering particles, roasted under vacuum at 375°C, and reacted in orthophosphoric acid at 90°C. The evolved CO_2 gas was analyzed on-line by a FISONS Prism isotope ratio mass spectrometer equipped with an automated preparation device at the University of California, Santa Cruz. Instrumental precision based on NBS-19 and Carrera Marble carbonate standards run daily was ±0.10‰ for $\delta^{18}O$ and ±0.05‰ for $\delta^{13}C$. All isotopic data are expressed using standard δ notation in per mil relative to the Peedee belemnite (PDB) carbonate standard (Table 1).

RESULTS

Oxygen isotopic data based on *C. mundulus* show two long-term cycles of 0.6‰ from 342 to 328 mbsf where $\delta^{18}O$ averaged 0.9‰, followed by a major increase of 1.2‰ from 328 to 323 mbsf (Fig. 2). After two subsequent decreases of 0.6‰, $\delta^{18}O$ averaged 1.2‰ from 320 to 310 mbsf, which was marked by numerous high-frequency fluctuations of ~0.5‰.

Carbon isotopic data also exhibited two long-term cycles of 0.5‰ from 342 to 326 mbsf where mean $\delta^{13}C$ increased by about 0.2‰. A

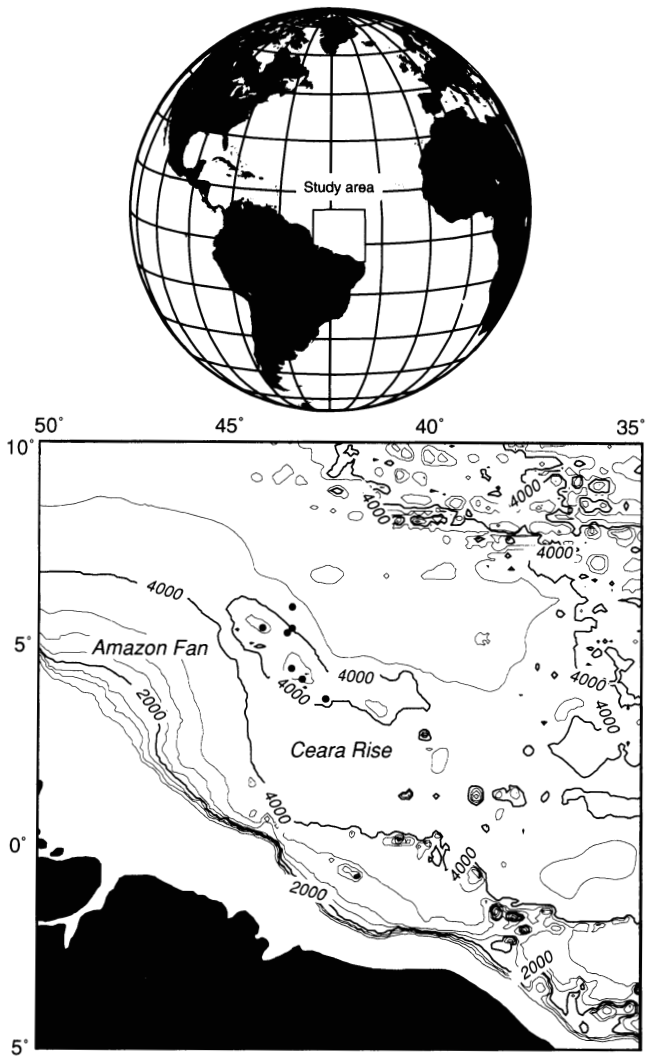

Figure 1. Location maps of Leg 154 drill site locations on Ceara Rise, western Equatorial Atlantic (contour interval 500 m).

large increase of 1‰ from 326 to 323 mbsf slightly lagged the $\delta^{18}O$ increase by about 1 m. After a subsequent decrease of 0.6‰, $\delta^{13}C$ averaged 1.2‰ from 320 to 310 mbsf, which was marked by numerous high-frequency fluctuations of 0.5‰.

DISCUSSION

Age Control

Recovery was nearly 100% in the four cores of Hole 929A that span the Oligocene/Miocene boundary. Several turbidites were found at Site 929, but these features are thin (10-cm scale) and their locations are known (Shipboard Scientific Party, 1995). All turbidites and slumps were meticulously identified and catalogued on board and were avoided during sampling. Age control for this site is based mainly on calcareous nannofossil and planktonic foraminifer biostratigraphy (Shipboard Scientific Party, 1995). Strontium isotopic data on planktonic foraminifers (Flower et al., this volume) improve the age control. Ages are according to the Leg 154 time scale (Curry, Shackleton, Richter, et al., 1995), which is based on the time scale of Cande and Kent (1992). The Cande and Kent time scales (1992, 1995) are not significantly different (<10 k.y.) in the 25–23 Ma interval.

Table 1. Stable isotopic and percent sand data for Hole 929A.

Core, section, interval (cm)	Depth (mbsf)	Depth (mcd)	Age (Ma)	% Sand (>63 μm)	$\delta^{13}C$ (‰)	$\delta^{18}O$ (‰)
154-929A-						
34X-1, 10–12	310.80	326.22	23.148	0.123	1.32	1.07
34X-1, 20–22	310.90	326.32	23.152	0.455	1.36	0.99
34X-1, 30–32	311.00	326.42	23.157	3.992	1.27	0.83
34X-1, 40–42	311.10	326.52	23.161	0.872	0.88	0.88
34X-1, 50–52	311.20	326.62	23.166	0.195	0.88	1.12
34X-1, 64–66	311.34	326.76	23.172	0.106	0.84	1.26
34X-1, 74–76	311.44	326.86	23.176	0.151	1.17	1.24
34X-1, 80–82	311.50	326.92	23.179	0.113	1.07	0.91
34X-1, 90–92	311.60	327.02	23.183	0.090	1.08	0.87
34X-1, 100–102	311.70	327.12	23.188	0.145	1.39	1.25

Only part of this table is produced here. The entire table appears on CD-ROM.

High-Resolution Stratigraphy

Sediment sampling at 10-cm intervals within calcareous nannofossil Zone CN1 and near the planktonic foraminifer Zone P22/N4 boundary provides high-resolution records (5-k.y. resolution) near the Oligocene/Miocene boundary, including the Antarctic glaciation represented by Mi1 (Fig. 3). The oxygen isotopic data show two long-term glacial cycles with a period of ca. 400 k.y. preceding Mi1. The maximum $\delta^{18}O$ value reached is 2.15‰; this rather high value (compared with much of the mid-Cenozoic; e.g., Wright and Miller, 1993) indicates significant East Antarctic ice volume at 23.65 Ma.

On long time scales (>100 k.y.) $\delta^{18}O$ covaries with $\delta^{13}C$ throughout the 24.8–23.1 Ma interval studied, suggesting a link between organic carbon burial and climate near the Oligocene/Miocene boundary (similar to the middle Miocene climatic transition; Woodruff and Savin, 1991; Flower and Kennett, 1993). However, the increases in

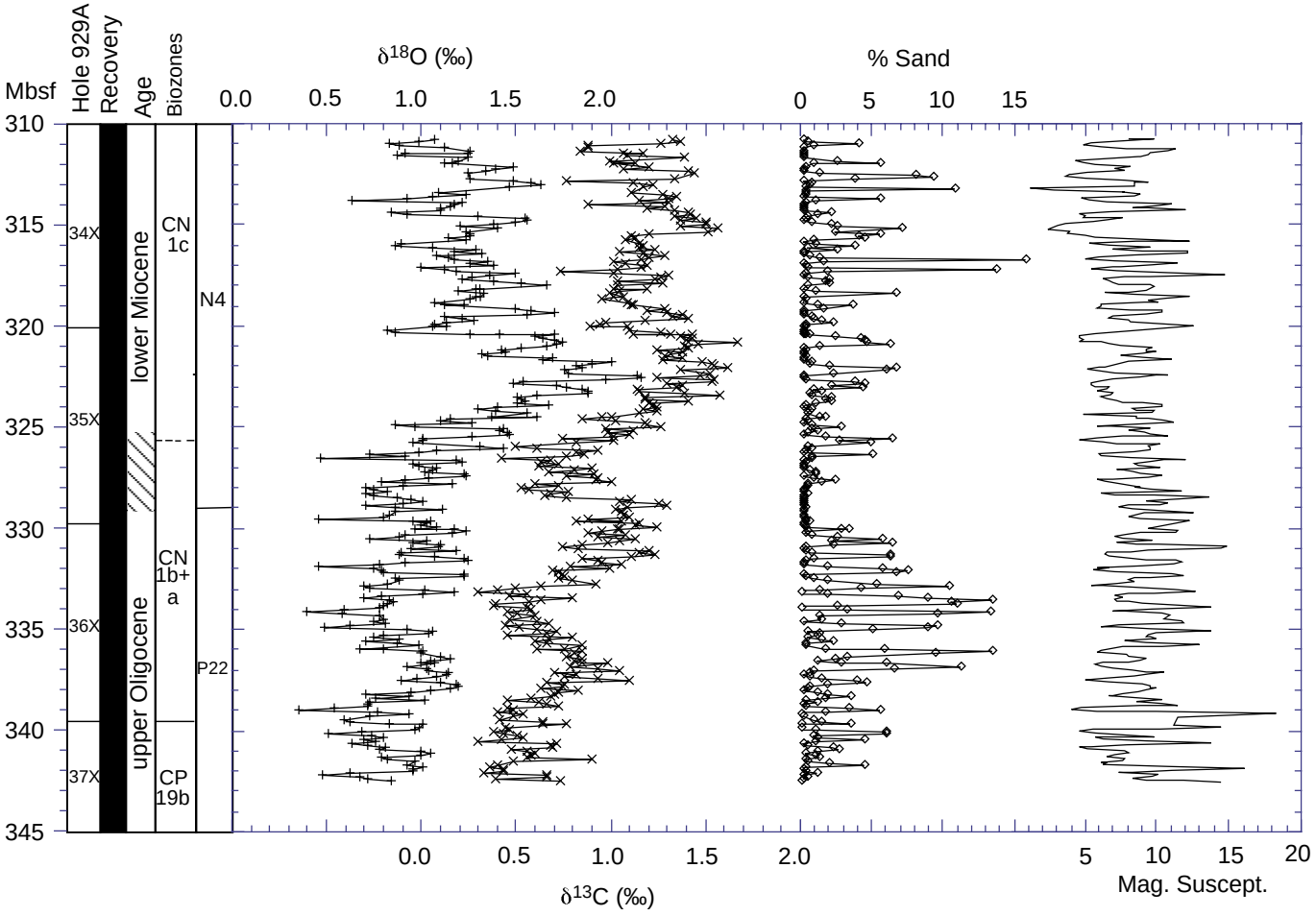

Figure 2. Oxygen and carbon isotopic, percent sand, and magnetic susceptibility data for Hole 929A vs. meters below sea floor (mbsf), spanning the Oligocene/Miocene boundary. Isotopic measurements were conducted on *Cibicidoides mundulus*. Core recovery is shown in black.

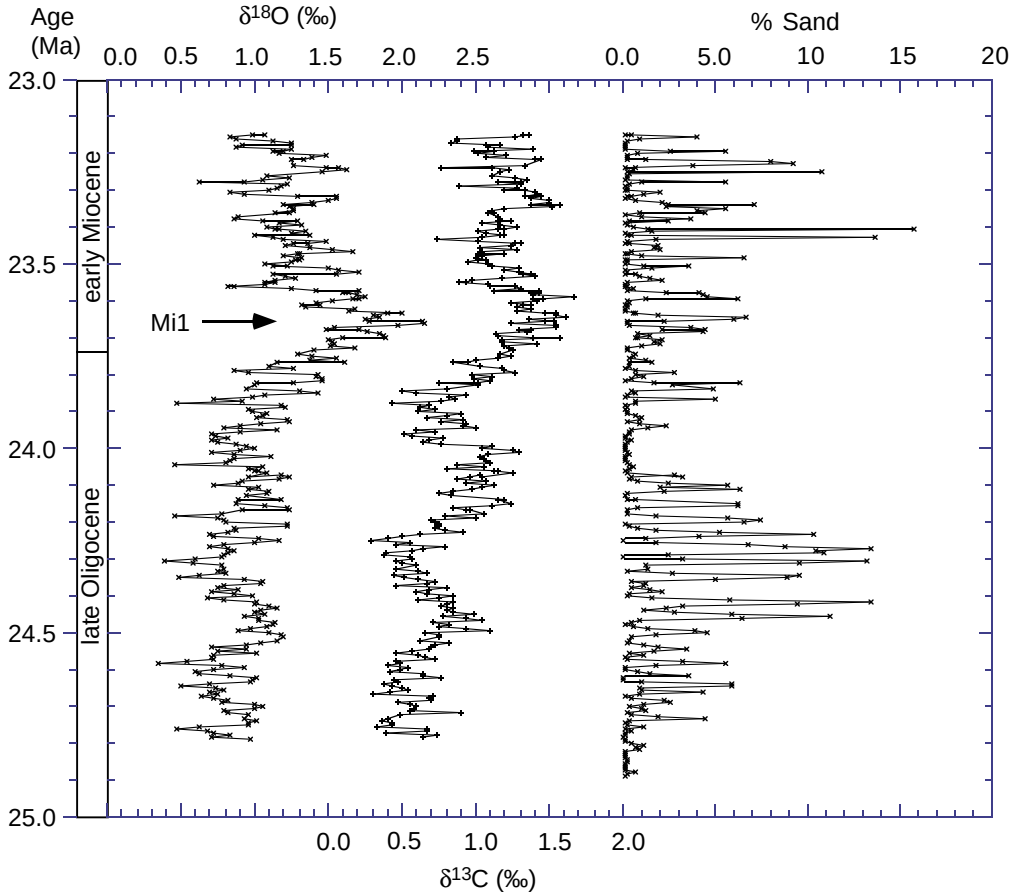

Figure 3. Oxygen, carbon isotopic, and percent sand records for Hole 929A, plotted vs. age (Ma), spanning the Oligocene/Miocene boundary. Isotopic measurements were conducted on *Cibicidoides mundulus.* Note the high-frequency cycle (~40 k.y.), superimposed on a lower-frequency cycle (~400 k.y.), in all records.

$\delta^{18}O$ slightly lead carbon isotopic increases by about 40 k.y., including the major $\delta^{18}O$ increase beginning at 23.9 Ma (Fig. 3). This observation could indicate that climatic change preceded changes in organic carbon burial in this interval by about 40 k.y. Additionally, each successive $\delta^{13}C$ maximum exhibits higher values, reaching 1.1‰ at 24.50 Ma, 1.3‰ at 24.02 Ma, and finally 1.6‰ at 23.65 Ma, when both $\delta^{18}O$ and $\delta^{13}C$ reached peak values.

These isotopic records better define the nature of Oligocene/Miocene $\delta^{18}O$ and $\delta^{13}C$ signals for stratigraphic correlation of marine and terrestrial sequences. In particular, the Mi1 $\delta^{18}O$ event of Miller et al. (1991) is shown to exhibit a gradual increase of 1.2‰ over 250 k.y. followed by two, rapid decreases of 0.6‰ within 20 k.y. at 23.62 and 23.57 Ma (Fig. 3). The $\delta^{13}C$ event associated with the Oligocene/Miocene boundary (CM O/M of Hodell and Woodruff, 1994) is shown to be the maximum in a series of at least three $\delta^{13}C$ cycles of the ca. 400-k.y. period, culminating at 23.65 Ma.

On shorter time scales (<100 k.y.) $\delta^{18}O$ and $\delta^{13}C$ do not appear to strongly covary. However, $\delta^{18}O$ does vary inversely with percent sand fraction, which is controlled mainly by foraminifer dissolution. Lower sand contents coincide with higher $\delta^{18}O$ values, suggesting that glacial intervals featured more corrosive bottom waters at Site 929 (Fig. 4). This relation is similar to that known for the late Quaternary, where corrosive Antarctic Bottom Water more strongly influences the deep western equatorial Atlantic during glacial intervals (e.g., Curry et al., 1988).

Milankovitch-Scale Periodicities

The stable isotopic time series exhibit Milankovitch-scale periodicity, with a range of periods. Both the $\delta^{18}O$ and $\delta^{13}C$ records exhibit a prominent long-term (ca. 400 k.y.) cycle, which probably indicates a long-term association between East Antarctic ice sheet variations and organic carbon burial/oxidation. This association has also been observed in middle Miocene (Woodruff and Savin, 1991; Flower and Kennett, 1993, 1995) and early Oligocene (Shackleton et al., 1984; Zachos et al., in press) deep-sea sequences. Superimposed on these long-term variations are high-frequency oscillations that are best studied by spectral analysis.

Spectral analysis is justified because inter-core gaps are small in this sequence. The uniform, well-lithified nature of the chalks in the Site 929 sequence allowed very little core material to be lost between cores obtained with the extended core barrel (XCB; Shipboard Scientific Party, 1995). Also, spectra based on shipboard multisensor systems track (MST) data (e.g., magnetic susceptibility) compare well with spectra based on downhole logging data (Shipboard Scientific Party, 1995).

Stable isotope and percent sand records were analyzed using standard techniques of spectral analysis, following Jenkins and Watts (1968). The records were linearly detrended, normalized, and resampled at a constant 4.4-k.y. spacing. Spectral densities were calculated based on 70 lags of the autocovariance function, for the entire 23.1–24.78 Ma interval (Fig. 4) and for the 24.0–24.78 Ma interval (Fig. 5).

In the 23.1–24.78 Ma interval, $\delta^{18}O$, $\delta^{13}C$, and percent sand feature a prominent spectral peak at the ca. 38-k.y. period (Fig. 4). The percent sand peak at 38-k.y. period is especially pronounced. All three spectra also exhibit lesser peaks in spectral density at about 23 k.y. In addition, the $\delta^{13}C$ spectra exhibit a strong 400-k.y. period, and the percent sand spectra feature significant peaks at 80 k.y. and 19 k.y.

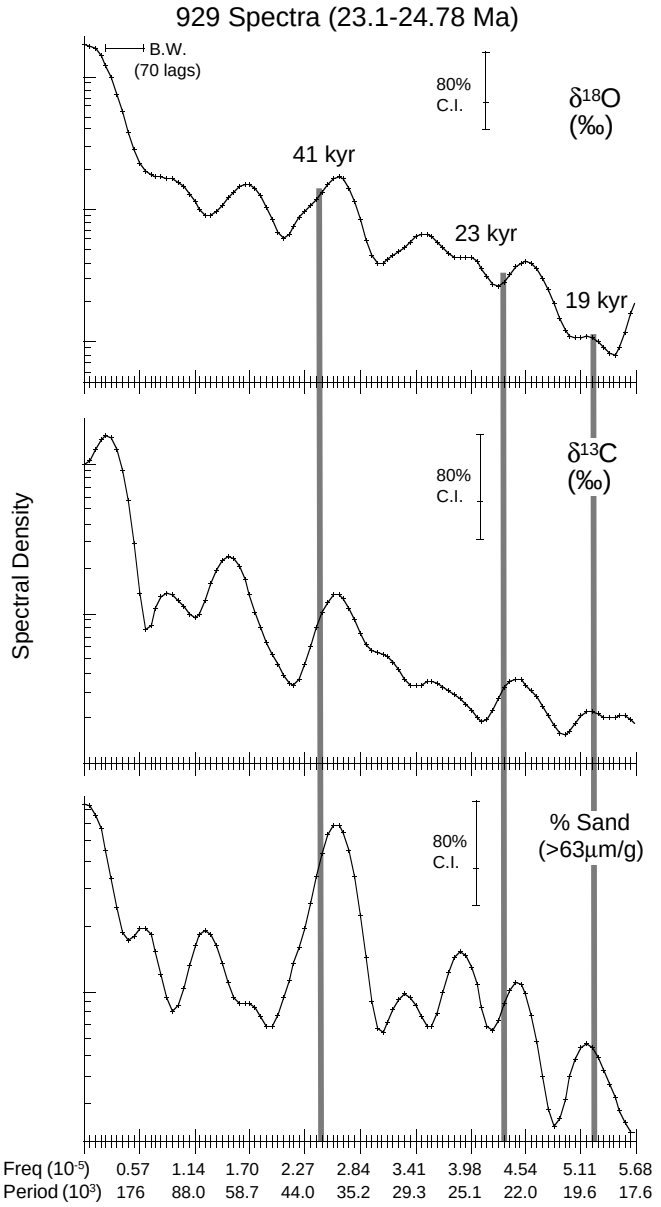

Figure 4. Power spectra for $\delta^{18}O$, $\delta^{13}C$, and percent sand (>63 µm/g) data from Hole 929A, for the 23.1–24.78 Ma interval. Note the strong peak in spectral density at about 38 k.y., common to all three records.

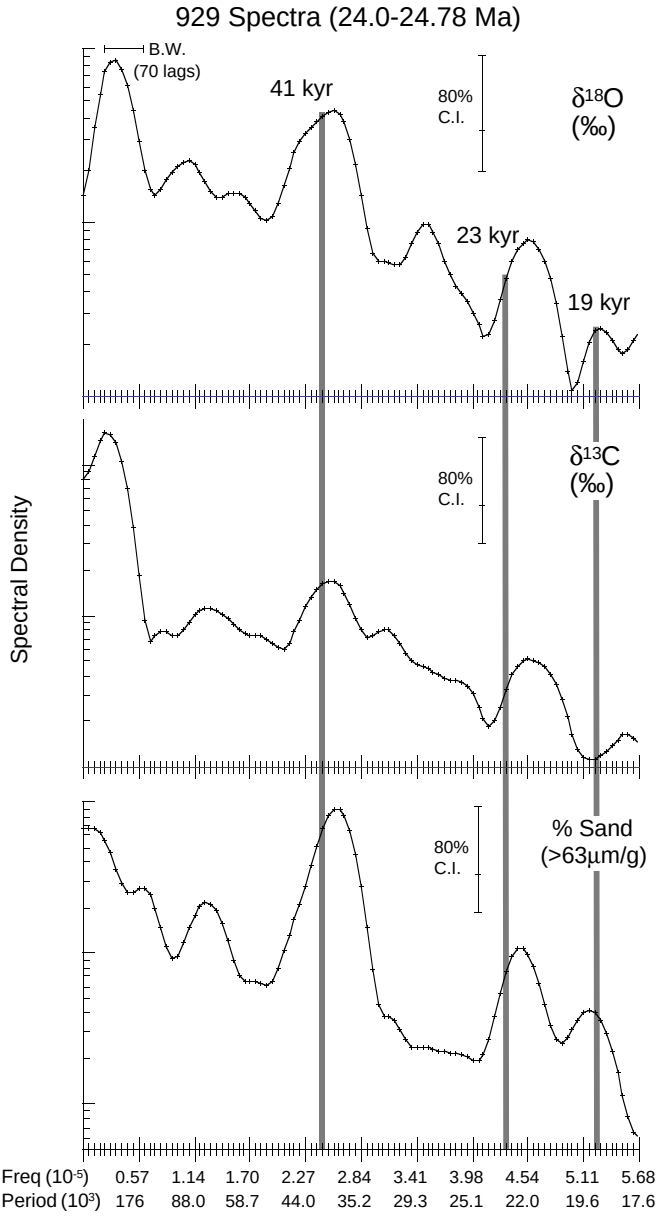

Figure 5. Power spectra for $\delta^{18}O$, $\delta^{13}C$, and percent sand (>63 µm/g) data from Hole 929A, for the 24.0–24.78 Ma interval. Note the strong peak in spectral density at about 41 k.y., common to all three records.

Higher-frequency spectral peaks are especially well-resolved in the 24.0–24.78 Ma interval. In this interval, $\delta^{18}O$, $\delta^{13}C$, and percent sand each feature prominent spectral peaks at the 40-k.y. and 22-k.y. periods (Fig. 5). In addition, the $\delta^{18}O$ and $\delta^{13}C$ spectra exhibit a strong 400-k.y. period.

A 41-k.y. period was also discerned in shipboard MST data (Shipboard Scientific Party, 1995), particularly magnetic susceptibility and percent reflectance. Magnetic susceptibility covaries inversely with percent sand, suggesting that magnetic susceptibility can be used as a proxy for carbonate content and possibly foraminifer test dissolution in this interval.

The dominance of a period close to obliquity (41 k.y.; especially in the 24.0–24.78 Ma interval) and eccentricity (400 k.y.) suggests a high-latitude control for these variations, because variations in obliquity have greatest effects on insolation in the high-latitude regions as a result of changing seasonality (e.g., Imbrie et al., 1992, 1993). A strong obliquity control of the $\delta^{18}O$ signal probably reflects East Antarctic ice sheet variability. This is a significant finding, as it supports an age for East Antarctic ice sheets greater than 24.8 Ma, consistent with evidence from ice-rafted debris records for a late Eocene-early Oligocene age (Barron et al., 1991; Breza and Wise, 1992; Zachos et al., 1992). It is also significant to find spectral evidence for East Antarctic ice sheet variations in the latest Oligocene, a time of relative global warmth. This finding suggests that intermittent East Antarctic ice sheets may have been present, even during intervals of relative global warmth.

Deep Atlantic Paleoceanography

Our high-resolution data near the Oligocene/Miocene boundary allow more detailed comparisons with previously published records from other ocean areas, particularly those that monitored Northern

and Southern Component Waters. Reconstruction of deep-water circulation patterns based on the $\delta^{13}C$ of benthic foraminifers at this time suggests a single southern deep-water source (SCW) and no significant Northern Component Water (NCW) source (Wright et al., 1992). This interpretation is based in part on finding the highest oceanic $\delta^{13}C$ values at Southern Ocean Site 704 (1.86‰) and lowest values at North Atlantic Site 553 (0.63‰; Wright et al., 1992).

High-resolution $\delta^{13}C$ records for Site 929 exhibit a maximum $\delta^{13}C$ value of 1.6‰ during Mi1, significantly lower than Site 704 (1.86‰). The south-to-north $\delta^{13}C$ gradient at 23.7 Ma suggests that SCW flowed north toward the equatorial Atlantic at this time. Thus, we confirm the suggestion of Wright et al. (1992) that Atlantic deep-water circulation during Mi1 near the Oligocene/Miocene boundary was dominated by a single SCW source, with no significant NCW.

CONCLUSIONS

Milankovitch-scale resolution (5-k.y. sampling) near the Oligocene/Miocene boundary allows better definition of the Mi1 $\delta^{18}O$ event. Mi1 is marked by a gradual increase of 1.2‰ over 250 k.y. from 23.9 to 23.6 Ma, followed by two rapid (ca. 20 k.y. each) decreases of 0.6‰ at 23.62 and 23.57 Ma.

The $\delta^{13}C$ maximum of 1.6‰ associated with the Oligocene/Miocene boundary is shown to be the last in a series of at least three $\delta^{13}C$ cycles of the ~400-k.y. period, culminating at 23.65 Ma. Strong low-frequency covariance between $\delta^{18}O$ and $\delta^{13}C$ is exhibited throughout the Oligocene/Miocene boundary sequence, suggesting a link between organic carbon burial and global climate change. An inverse relation between $\delta^{18}O$ and percent sand suggests more corrosive deep waters during glaciations, similar to that observed during the late Quaternary (e.g., Curry et al., 1988).

Spectral analysis of the $\delta^{18}O$, $\delta^{13}C$, and percent sand (>63 µm/g) records documents a dominant peak in spectral density in each parameter at 40-k.y., especially in the 24.0–24.78 Ma interval. In addition, $\delta^{18}O$ and $\delta^{13}C$ exhibit a strong peak at the ~400-k.y. period. Dominant spectral density peaks at obliquity and eccentricity periods suggest a high-latitude control, probably East Antarctic ice sheet variability. Indeed, a strong 40-k.y. period in the 24.0–24.78 Ma interval suggests East Antarctic ice sheet variability in the latest Oligocene prior to Mi1, during an interval of relative global warmth.

The $\delta^{18}O$ maximum was reached (~2.15‰), and the presence of obliquity and eccentricity periods in oxygen isotopic records are consistent with East Antarctic ice sheet variability near the Oligocene/Miocene boundary. Antarctic glaciation near the Oligocene/Miocene boundary was associated with a strong SCW source that reached the deep western equatorial Atlantic.

ACKNOWLEDGMENTS

This work was supported by the JOI/USSSP (154-208396) along with partial support from NSF (OPP-9423485 to B.P.F. and OCE-9458367 to J.C.Z). We thank the Ocean Drilling Program for providing samples; J. D. Wright and an anonymous reviewer for constructive reviews; and Todd Green, Peter Heitz, and Kathy Vencill for laboratory assistance.

REFERENCES

Barker, P.F., and Burrell, J., 1977. The opening of the Drake Passage. *Mar. Geol.*, 25:15–34.

Barrett, P.J., Hambrey, M.J., Harwood, D.M., Pyne, A.R., and Webb, P.-N., 1989. Synthesis. *In* Barrett, P.J. (Ed.), *Antarctic Cenozoic History from the CIROS-1 Drillhole, McMurdo Sound.* DSIR Bull. N.Z., 245:241–251.

Barron, J., Larsen, B., and Baldauf, J.G., 1991. Evidence for late Eocene to early Oligocene Antarctic glaciation and observations on late Neogene glacial history of Antarctica: results from Leg 119. *In* Barron, J., Larsen, B., et al., *Proc. ODP, Sci. Results*, 119: College Station, TX (Ocean Drilling Program), 869–891.

Berger, A., 1977. Long-term variations of the earth's orbital elements. *Celest. Mech.*, 15:53–74.

Breza, J.R., and Wise, S.W., Jr., 1992. Lower Oligocene ice-rafted debris on the Kerguelen Plateau: evidence for East Antarctic continental glaciation. *In* Wise, S.W., Jr., Schlich, R., et al., *Proc. ODP, Sci. Results*, 120: College Station, TX (Ocean Drilling Program), 161–178.

Broecker, W.S., and van Donk, J. 1970. Insolation changes, ice volumes, and the O^{18} record in deep-sea cores. *Rev. Geophys. Space Phys.*, 8:169–198.

Cande, S.C., and Kent, D.V., 1992. A new geomagnetic polarity time scale for the Late Cretaceous and Cenozoic. *J. Geophys. Res.*, 97:13917–13951.

————, 1995. Revised calibration of the geomagnetic polarity timescale for the Late Cretaceous and Cenozoic. *J. Geophys. Res.*, 100:6093–6095.

Ciesielski, P.F., and Wise, S.W., Jr., 1977. Geologic history of the Maurice Ewing Bank of the Falkland Plateau (southwest Atlantic sector of the Southern Ocean) based on piston and drill cores. *Mar. Geol.*, 35:175–207.

Curry, W.B., Duplessy, J.C., Labeyrie, L.D., and Shackleton, N.J., 1988. Changes in the distribution of $\delta^{13}C$ of glacial deep water ΣCO_2 between the last glacial and the Holocene. *Paleoceanography*, 3:317–341.

Curry, W.B., Shackleton, N.J., Richter, C., et al., 1995. *Proc. ODP, Init. Repts.*, 154: College Station, TX (Ocean Drilling Program).

Fairbanks, R.G., and Matthews, R.K., 1978. The marine oxygen isotope record in Pleistocene coral, Barbados, West Indies. *Quat. Res.*, 10:181–196.

Flower, B.P., and Kennett, J.P., 1993. Middle Miocene ocean/climate transition: high-resolution oxygen and carbon isotopic records from DSDP Site 588A, Southwest Pacific. *Paleoceanography*, 8:811–843.

————, 1995. Middle Miocene deepwater paleoceanography in the southwest Pacific: relations with East Antarctic Ice Sheet development, *Paleoceanography*, 10:1095–1113.

Hays, J.D., Imbrie, J., and Shackleton, N.J., 1976. Variations in the Earth's orbit: pacemaker of the ice ages. *Science*, 194:1121–1132.

Hodell, D.A., and Woodruff, 1994. Variations in the strontium isotopic ratio of seawater during the Miocene: stratigraphic and geochemical implications. *Paleoceanography*, 9:405–426.

Imbrie, J., Berger, A., Boyle, E., Clemens, S., Duffy, A., Howard, W., Kukla, G., Kutzbach, J., Martinson, D., McIntyre, A., Mix, A., Molfino, B., Morley, J., Peterson, L., Pisias, N., Prell, W., Raymo, M., Shackleton, N., and Toggweiler, J., 1993. On the structure and origin of major glaciation cycles, 2. The 100,000-year cycle. *Paleoceanography*, 8:699–735.

Imbrie, J., Boyle, E.A., Clemens, S.C., Duffy, A., Howard, W.R., Kukla, G., Kutzbach, J., Martinson, D.G., McIntyre, A., Mix, A.C., Molfino, B., Morley, J.J., Peterson, L.C., Pisias, N.G., Prell, W.L., Raymo, M.E., Shackleton, N.J., and Toggweiler, J.R., 1992. On the structure and origin of major glaciation cycles, 1. Linear responses to Milankovitch forcing. *Paleoceanography*, 7:701–738.

Imbrie, J., Hays, J.D., Martinson, D.G., McIntyre, A., Mix, A.C., Morley, J.J., Pisias, N.G., Prell, W.L., and Shackleton, N.J., 1984. The orbital theory of Pleistocene climate: support from a revised chronology of the marine $\delta^{18}O$ record. *In* Berger, A., Imbrie, J., Hays, J., Kukla, G., and Saltzman, B. (Eds.), *Milankovitch and Climate* (Pt. 1), NATO ASI Ser. C, Math Phys. Sci., 126: Dordrecht (D. Reidel), 269–305.

Jenkins, G.M., and Watts, D.G., 1968. *Spectral Analysis and Its Applications:* San Francisco (Holden Day).

Keigwin, L.D., 1987. Toward a high-resolution chronology for latest Miocene paleoceanographic events. *Paleoceanography*, 2:639–660.

Kennett, J.P., 1977. Cenozoic evolution of Antarctic glaciation, the circum-Antarctic Ocean, and their impact on global paleoceanography. *J. Geophys. Res.*, 82:3843–3860.

Lawver, L., 1992. The development of paleoseaways around Antarctica. *In* Kennett, J.P., and Warnke, D.A. (Eds.), *The Antarctic Paleoenvironment: A Perspective on Global Change, Part I.* Am. Geophys. Union, Antarct. Res. Ser., 56:7–30.

Leckie, R.M., and Webb, P.N., 1983. Late Oligocene-early Miocene glacial record of the Ross Sea, Antarctica: evidence from DSDP Site 270. *Geology*, 11:578–582.

Mesolella, K.J., Matthews, R.K., Broecker, W.S., and Thurber, D.L., 1969. The astronomical theory of climatic change: Barbados data. *J. Geol.*, 77:250–274.

Miller, K.G., and Fairbanks, R.G., 1985. Oligocene to Miocene carbon isotope cycles and abyssal circulation changes. *In* Sundquist, E.J., and Bro-

ecker, W.S. (Eds.), *The Carbon Cycle and Atmospheric CO_2: Natural Variations Archean to Present.* Geophys. Monogr., Am. Geophys. Union, 32:469–486.

Miller, K.G., Feigenson, M.D., Kent, D.V., and Olsson, R.K., 1988. Upper Eocene to Oligocene isotope ($^{87}Sr/^{86}Sr$, $\delta^{18}O$, $\delta^{13}C$) standard section, Deep Sea Drilling Project Site 522. *Paleoceanography,* 3:223–233.

Miller, K.G., Wright, J.D., and Brower, A.N., 1989. Oligocene to Miocene stable isotope stratigraphy and planktonic foraminifer biostratigraphy of the Sierra Leone Rise (DSDP Site 366 and ODP Site 667). *In* Ruddiman, W., Sarnthein, M., et al., *Proc. ODP, Sci. Results,* 108: College Station, TX (Ocean Drilling Program), 279–294.

Miller, K.G., Wright, J.D., and Fairbanks, R.G., 1991. Unlocking the Ice House: Oligocene-Miocene oxygen isotopes, eustasy, and margin erosion. *J. Geophys. Res.,* 96:6829–6848.

Pisias, N.G., and Mix, A.C., 1988. Aliasing of the geologic record and the search for long-period Milankovitch cycles. *Paleoceanography,* 3:613–619.

Pisias, N.G., Shackleton, N.J., and Hall, M.A., 1985. Stable isotope and calcium carbonate records from hydraulic piston cored Hole 574A: high-resolution records from the middle Miocene. *In* Mayer, L., Theyer, F., Thomas, E., et al., *Init. Repts. DSDP,* 85: Washington (U.S. Govt. Printing Office), 735–748.

Prentice, M.L., and Matthews, R.K., 1988. Cenozoic ice-volume history: development of a composite oxygen isotope record. *Geology,* 16:963–966.

Raymo, M.E., Ruddiman, W.F., Backman, J., Clement, B.M., and Martinson, D.G., 1989. Late Pliocene variation in Northern Hemisphere ice sheets and North Atlantic deep water circulation. *Paleoceanography,* 4:413–446.

Ruddiman, W.F., Raymo, M.E., Martinson, D.G., Clement, B.M., and Backman, J., 1989. Pleistocene evolution: Northern Hemisphere ice sheets and North Atlantic Ocean. *Paleoceanography,* 4:353–412.

Shackleton, N.J., Hall, M.A., and Boersma, A., 1984. Oxygen and carbon isotope data from Leg 74 foraminifers. *In* Moore, T.C., Jr., Rabinowitz, P.D., et al., *Init. Repts. DSDP,* 74: Washington (U.S. Govt. Printing Office), 599–644.

Shipboard Scientific Party, 1995. Site 929. *In* Curry, W.B., Shackleton, N.J., Richter, C., et al., *Proc. ODP, Init. Repts.,* 154: College Station, TX (Ocean Drilling Program), 337–417.

Tucholke, B.E., and Mountain, G.S., 1979. Seismic stratigraphy, lithostratigraphy, and paleosedimentation patterns in the North American Basin. *In* Talwani, M., Hay, W., and Ryan, W.B.F. (Eds.), *Deep Drilling Results in the Atlantic Ocean: Continental Margins and Paleoenvironment.* Am. Geophys. Union, Maurice Ewing Ser., 3:58–86.

Woodruff, F., and Savin, S.M., 1991. Mid-Miocene isotope stratigraphy in the deep-sea: high resolution correlations, paleoclimatic cycles, and sediment preservation. *Paleoceanography,* 6:755–806.

Wright, J.D., and Miller, K.G., 1992. Miocene stable isotope stratigraphy, Site 747, Kerguelen Plateau. *In* Wise, S.W., Jr., Schlich, R., et al., *Proc. ODP, Sci. Results,* 120: College Station, TX (Ocean Drilling Program), 855–866.

————, 1993. Southern Ocean influences on late Eocene to Miocene deepwater circulation. *In* Kennett, J.P., and Warnke, D.A. (Eds.), *The Antarctic Paleoenvironment: A Perspective on Global Change, Part II.* Antarct. Res. Ser., 60:1–25.

Wright, J.D., Miller, K.G., and Fairbanks, R.G., 1992. Early and middle Miocene stable isotopes: implications for deepwater circulation and climate. *Paleoceanography*, 7:357–389.

Zachos, J.C., Quinn, T.M., and Salamy, K.A., 1996. High-resolution (10^4 years) deep-sea foraminiferal stable isotope records of the Eocene-Oligocene climate transition. *Paleoceanography,* 11:251–266.

Zachos, J.C., Rea, D.K., Seto, K., Niitsuma, N., and Nomura, R., 1992. Paleogene and early Neogene deep water history of the Indian Ocean: inferences from stable isotopic records. *In* Duncan, R.A., Rea, D.K., Kidd, R.B., von Rad, U. and Weissel, J.K. (Eds.), *The Indian Ocean: A Synthesis of Results from the Ocean Drilling Program.* Am. Geophys. Union, Geophys. Monogr., 70:351–386.

Zahn, R., and Diester-Haass, L., 1995. Orbital forcing of Eocene-Oligocene climate: high resolution records of benthic isotopes from ODP Site 689, Maud Rise. *ICP V Progr. Abstr., 5th Int. Conf. Paleoceanogr., Halifax,* 177.

Date of initial receipt: 1 December 1995
Date of acceptance: 6 May 1996
Ms 154SR-141